

DESIGN AND CONSTRUCTION OF MAGNETIC MEASUREMENTS
IN A HIGH PERFORMANCE SPECTROMETER MAGNET.

B. Turck

Département du Synchrotron Saturne,
CEN/Saclay (France).

Abstract

The influence of every kind of measuring error was tested directly on the image through a trajectory program. This work points out on which parts of the equipment the accuracy must be high or may be low. A Hall probe system was built to measure the field map of the 1 GeV spectrometer magnet. A 0.4 mm image width was achieved after shimming, that is to say an overall accuracy better than 10^{-4} for $\Delta p/p_0$.

The natural trend is to look for the maximum accuracy out of the measurement system. This attitude is generally not justified if it is noticed that in the interpretation of a spectrometry experience, the principal parameters are the dispersion and the aberration but not the absolute positions of the images. Likewise the performances are strongly depending on the nature of the errors. It is necessary to solve the following problem in a general way. What are the qualities to ask the field measurements to obtain the essential properties of this optical system that is, to appreciate a difference between the momenta of two beams. That work points out, in the same way, for an expected accuracy the most economical conditions to design and construct these magnetic measurements.

I. Principles

In the experience the results are used by a trajectory program. Measurement error or mispositioning of the probe deal only with the separation of two images or the dispersion. Besides, a too general analysis of the error effects may neglect compensation¹ and leads to ask the measurements a too high precision.

Practically, magnetic measurements are asked to give the field map of the magnet in order to be able to correct this field with a shimming. The overall map next to this shimming must approach the ideal expected one.

This field must be such in our experience that in the plane of the target two spots corresponding to momenta p_0 and $p_0 + \Delta p$ must not lead in any way to an overall error greater than 10^{-4} . The method consists in simulating the real case. After making the inventory of all kinds of possible errors (amplitude, nature), the program takes in account the theoretical field values on a polar mesh and assigns to each point of this mesh either the "perturbated" field or the altered position of the point by the tested kind of error.

The magnet is the spectrometer used for the 1 GeV spectrometry experimentation at the proton accelerator Saturne in Saclay^{2,3} (fig. 1).

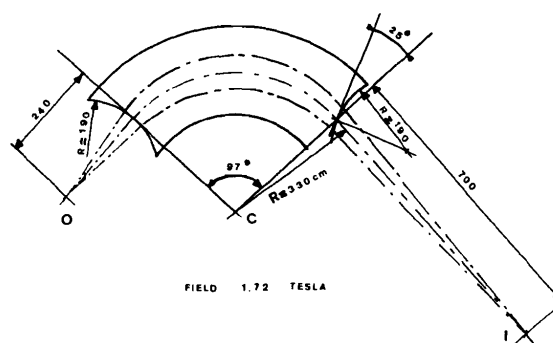


FIG. 1

Fig. 1. The magnet and the optical conditions.

To limit somewhat the problem we decide.

1) To measure the field only in the median plane. That reduces the problem to small vertical acceptance beams. But if it is necessary to get the vertical aberrations it is possible to develop $B(x, s, z)$ in the neighbourhood of the plane $z = 0$.

2) To use a Hall probe which seems to be well fitted to a point to point cartography.

3) To measure the fields inside and outside (fringe field) of the sector with the same polar system.

II. Measuring errors

The probe is a temperature regulated Hall plate. All kinds of errors may be summed up as follows in Table 1, according to their origins.

TABLE 1

| Error | RANDOM | | SYSTEMATIC | | DRIFT | |
|--------------------|--------|------|------------|------|-------|------|
| | Abs. | Rel. | Abs. | Rel. | Abs. | Rel. |
| Temp ^{re} | | Yes | | Yes | | |
| Calib ⁿ | | | Yes | | | |
| Supply | | Yes | | Yes | | Yes |
| DVM | Yes | | Yes | Yes | Yes | Yes |

If we consider as drift, a variation with time during the field mapping, differences due to a drift during the period between the calibration and the mapping are considered as systematic errors.

III. Influence of measurement errors

The magnet parameters were adjusted any way inside and in the fringe field so as to get through an ideal map for a 3 trajectories beam, issued from the same object point a punctual image AB (< 0.002 mm), (fig. 2). According to the wedged and curved faces, it is sufficient to adjust the β parameter to -0.776 in the radial law of the field in the cross section.

$$B = B_0 \left(1 + \beta \left(\frac{x}{\rho} \right)^2 \right)$$

We desire to separate two images corresponding to momenta p_0 and $p_0(1 + \frac{\Delta p}{p_0})$ with $p_0 = 1.4$ GeV/c and $\Delta p/p_0 = 10^{-4}$.

According to the magnet performances these two images are 1.44 mm distant in the focal plane.

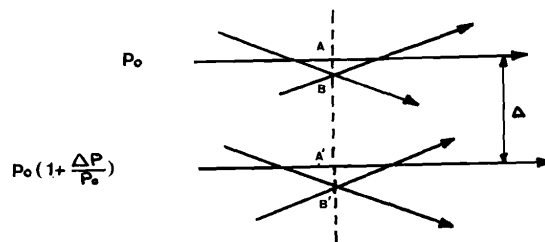


FIG 2

Fig. 2. The dispersion and the images.

The separation is possible if the sizes of the spots AB and A'B' are small compared with the dispersion Δy . Introducing field errors of different natures and amplitudes will alter both the position of the central orbit (null incidence angle), what we call the displacement and the spot sizes. The action of these errors are compared with the initial dispersion Δy (1.44 mm for 10^{-4}).

Each of these errors was tested⁴, so we can give here only 3 examples and the essential conclusions.

1. Influence of a relative systematic error :

We change locally the true field values with a relative error such as B_i becomes $B = B_i (1 + \frac{\Delta B}{B_i})$.

It can be seen on Table 2, that a relative systematic error keeps quite unaltered the separation power of the spectrometer.

TABLE 2

| Systematic relative error $\frac{\Delta B}{B_i}$ | Displacement mm | Spot size mm |
|--|-----------------|--------------|
| 10^{-5} | - 0.144 | + 0.001 |
| 10^{-4} | - 1.443 | + 0.001 |
| 10^{-3} | - 14.412 | - 0.002 |

2. Influence of relative random errors :

The field value at each point of the polar mesh is assigned with a relative

random error drawn out of a practically Gaussian population of square mean root $\sigma(\epsilon_B)$. For each map, orbits are such that displacement are distributed according to a Gaussian law around a mean null value. Through a good number of tests, the variances σ^2 of the displacement and spot size can be estimated. For a fluctuation of field value $\sigma(\epsilon_B) = 5 \cdot 10^{-4}$ with $B = B_i (1 + \epsilon_B)$ we obtain :

TABLE 3

| Relative random error | Image displacement mm | Image width mm |
|--|--------------------------|---------------------|
| $\sigma(\epsilon_B) = 5 \cdot 10^{-4}$ | $\sigma(\delta) = 0.360$ | $\sigma(t) = 0.400$ |

Therefore, though the error effect is smoothed because of its random nature, there stays on the image an unnegligible aberration. The reason for this is that the field values used along each orbit for the trajectory calculation are perturbed by quite independent errors.

3. Influence of measurement apparatus drifts :

In a magnet with large azimuthal extent, if the collection of field values is made along the beam direction, the apparatus drifts may introduce on the integrals $\int B ds$ along two quasi parallel orbits practically independent errors. This effect becomes bigger when the measuring time is high and the drift law far from a linear one. Consequently, it is more interesting to carry out the mapping along a radial direction (perpendicular to the beam).

This brings two principal advantages:

- The time is limited to the radial way one.
- The drift effects is distributed over every trajectory.

Thus, only the "mean drift" effect on each radial way has an effect. If, a drift is considered as being a random phenomenon superimposed to a slowly changing mean value without any particular law of linear type, it leads to a modification of the field integrals along the corresponding trajectories and to aberrations at the image. It can be seen that a drift linear with time does not introduce any aberration. The reason is, that a linear drift is equivalent with a field gradient : so we get a displacement without any extra aberration.

Therefore, aberrations proceed from errors on the differences between the field integrals along several trajectories being parties to the construction of the image. We realize that if through the measuring process, errors at each measurement points are not independent the error on the differences $\Delta \int B ds$ and the overall effect on the image may be particularly small, even negligible.

III. Influence of positioning errors

Likewise, it is possible to inject in the program, errors coming from the positioning equipment. Mechanical imprecisions or position reading result in errors of different nature and amplitude.

We give, as an example, three kinds of errors, all the effects were reported in a previous work.⁵

1. Systematic error on the sector angle :

This is an azimuthal systematic error appearing when we get the field mapping for the two magnet halves. It subsists an imprecision inside the magnet where the two halves have to join. That corresponds to an error on the value $\int B ds$ or on the value of the magnetic length of the magnet.

TABLE 4

| Angle error radian | Displacement mm | Spot width mm |
|--------------------|-----------------|---------------|
| 10^{-5} | 0.072 | + 0.003 |
| 10^{-4} | 0.715 | + 0.006 |
| 10^{-3} | 7.181 | - 0.033 |

2. Nonlinearity of the slide bar :

This nonlinearity involves a systematic however radially localized error (fig. 3). Therefore the effects are different on each trajectory. That kind of error introduces large aberrations. A 0.1 mm nonlinearity results in an 0.130 mm image width.

3. Random azimuthal errors :

. If mapping is made with moving along circles, the error is done independently on each point. A fluctuation $\sigma(\epsilon) \approx 0.3$ mm on each point results in a 0.2 mm aberration.

. If, as we propose the measurements are collected along polar radius, the aberration is only 0.04 mm for the maximum emittance of the beam (60 mrad).

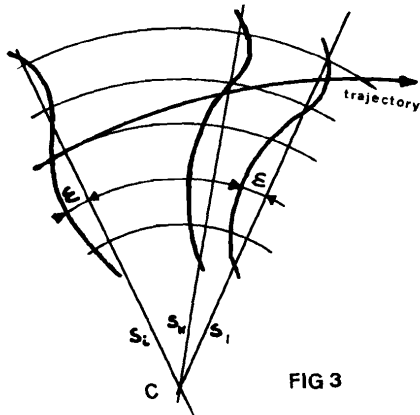


Fig. 3. Case of an unrectilignity on the slide-bar.

IV. Synthesis of the error effects

If the systematic measuring errors, related point to point, by a linear law, influence the image position, they don't alter its size. On the contrary, any random errors, drifts and radially located systematic errors act directly on the image width. This later kind of error introduces large aberrations on the one hand because of their systematic aspect and on the other hand because of their located type. There is no typically random ponderation and this defect acts all along the orbit in the fringe fields. Moreover, their radially located nature is such here that independency between local errors along a polar radius introduces defects on the $\Delta \int Bds$ integrals between trajectories and therefore image aberrations.

Practically, during a measuring run may be all the mentioned errors not present. Depending on the chosen system and the movement direction, such and such an error may not appear. We showed, that it was of a great interest, to collect the map along a radial direction (perpendicular to the beam). That leads to two principal advantages :

- drift effects are distributed and in part compensated.
- azimuthal errors are also distributed on every trajectory, introducing small effects on the image.

V. Application to the precisions asked out of the system

After such a complete study, it is possible to determine with minimum errors, mechanical precision to ask such and such a part of the system. Besides, that allows to distribute the errors and to demand high performances only where they are absolutely necessary. That way defines the most fitted and most economical system.

If the principle of a radial movement is chosen, it is possible to calculate tolerances on every part of the system. If an 0.4 mm aberration is accepted, (that is the third of the dispersion in the focal plane), because of the great number of error natures, and because of their independency we write :

$$\sum (\alpha_i t_i)^2 < 0.4 \text{ mm}$$

t_i is the aberration appearing from the error of type i , of unity amplitude and α_i is the actual amplitude.

All these errors have not the same effects and the biggest ones are looked for being minima¹.

That leads us :

1) To make a slide-bar with machining on the rectilignity, and constancy of the step of ± 0.07 mm. Other tolerances are about 0.3 mm in particular the azimuthal tolerances. That justifies to read the azimuthal position on an angle measuring system, located at the sector magnet centre, the Hall probe being 3.30 m far from it.

2) On the measuring part, to take care of :

- random errors to limit to 2.10^{-4}
- drifts to limit to 2.10^{-4} during a radial way.

VI. The carriage mechanism

The probe moves in the whole median plane inside the sector and outside in the fringe field with a polar reference system, the centre of which is the curvature centre of the reference orbit.

The magnet size assigns the mechanism, rigidity and length constraints which lead to make independently the mapping on each magnet half. That allows to use a straight arm. The framework made up of a three arms

system with counterweights, joins the measuring probe to the pivot. (fig. 4)

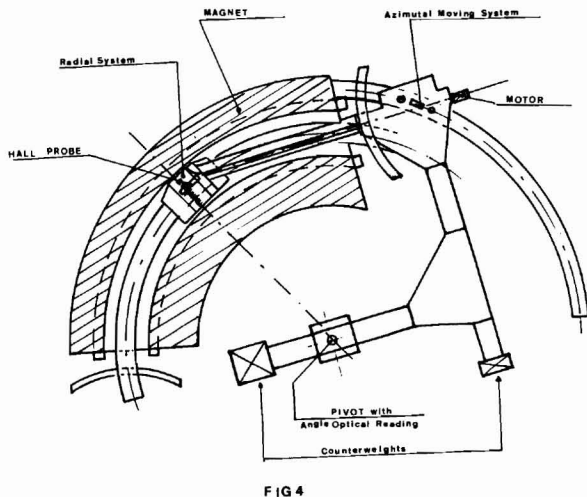


FIG 4

Fig. 4. Measuring equipment.

The probe carrier is automatically moved by means of a motor put outside of the field. This motor drives a screw coupled to the probe carrier system. The screw is machined in such a way that with a continuous motor rotation, for one half turn the probe moves and for the other half turn it stands still. By that means regular and constant steps can be achieved. The motor speed variation provides a fine adjustment of the time between two measurements. (fig. 5)



Fig. 5. Radial moving system.

Measure is always carried out in the same outwards direction. The coming back movement of the carrier is quicker and happens during the azimuthal motion. This one is obtained by an hydropneumatic system. The steps are 20 mm and are constant with an accuracy of 0.2 mm. But, when the system is still the location of the measurement point is known with a + 0.05 precision by means of an optical reader (designer J. Heidenhain), delivering 360 000 positioning pulses per turn (360°).

VII. The measuring system

The local field measure is achieved by a FC 32 Hall probe, which is electrically temperature regulated. The temperature sensor is a thermistance encapsulated with the probe in a copper block surrounded with a plexiglass box. This thermistance is in series with another one placed outside. This one of small value is supplied with an indirect heating coupled to the block one⁶. Thus, the thermal fluctuation and the regulations period are strongly reduced down to ± 0.03°C and 2 seconds. The Hall probe was selected, after a one month aging in a field, among five FC 32, which didn't drift much with time.

In order to strongly limit the slow drift effect of the voltmeter, we chose to collect for each point successively the Hall voltage and the supply current of the probe on a shunt resistor, by the same voltmeter (VIDAR 521) in the same voltage range (0.1 V), and then to evaluate each measurement in relation to the first current one (V_{io}).

That way eliminates to a great extent, drift effects coming from the current supply and from the voltmeter⁷.

The used voltage is :

$$V_{Hu} = V_{Hm} \frac{V_{vo}}{V_{im}}$$

If the voltmeter gets a drift the voltage becomes :

$$V'_{Hu} = V_{io} \frac{V_{Hm} + \Delta V_m}{V_{im} + \Delta im}$$

It can be seen that if V_H and V_i are of the same order of magnitude, hence it follows a quasi-compensation of the voltmeter drift error.

Moreover, an oscillator of a RMN system measures inside the sector the present reference field and delivers a frequency f_m relating to this reference field.

The voltage used in the orbit program is :

$$V_{Hf} = V_{Hm} \frac{V_{i0}}{V_{im}} \frac{F_0}{F_m}$$

The calibrating curve of the probe is given by means of a polynomial of the 13th degree development. The smoothing of this curve was good to ± 0.2 gauss between 0 and 2 teslas.

Long time tests about dispersion of the Hall ponderated voltage, dispersion due to various fluctuations (temperature, power supply, voltmeter, etc...) resulted in an evaluation of this overall dispersion of $\pm 4.10^{-5}$ in a random aspect. That is, corresponding to the necessary tolerances.

VIII. The sequence and data recording

Measuring, collecting, azimuthal and radial motions are programed and the whole sequence is automatic. A data transducer, in series with the voltmeter and frequency meter drives a card puncher. On each card, all the informations corresponding to two points are punched i - e radial and azimuthal positions, Hall voltage, Hall current, resonance frequency.

The mean duration between two points is 4 seconds and the mapping of one half of the magnet obtained in 3 hours (fig.6)

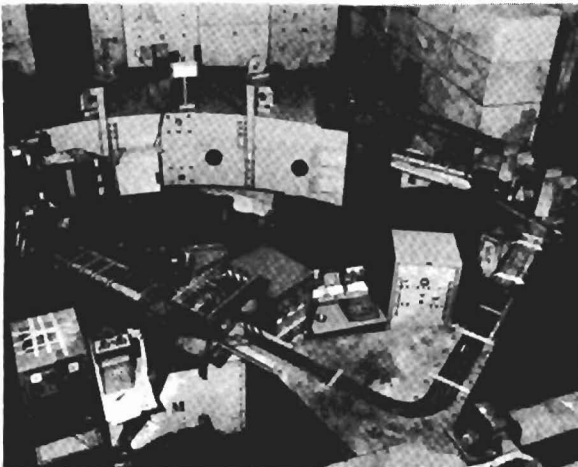


Fig. 6. Measuring equipment during a run.

IX. Results

All these informations are compiled by a trajectory program after getting the field out of the ponderated hall voltage.

The first measurements make us sure of the quality of the magnet by comparison with the magnetic study calculations?

In a cross section the field is close to the theoretical one with an accuracy better than 10^{-4} (fig. 7).

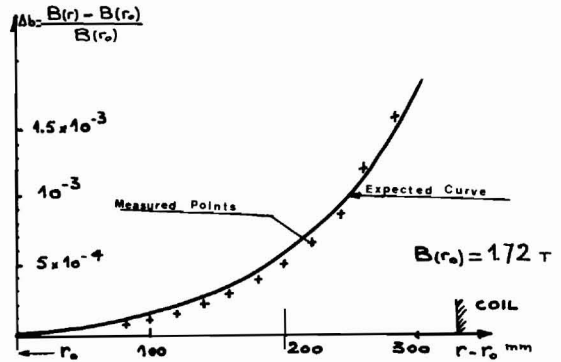


FIG 7

Fig. 7. Magnetic field curve measured in a cross section.

The magnetic lengths are such that the curvature radius at the ends are achieved with a 1% precision, that is to say a magnetic length evaluated with a 0.05 mm accuracy.¹⁰

The whole map is then used to determine the shimming necessary to get an ideal map, conditional to a fine focalization. These shims were calculated, put inside the sector and in the fringe field. Then a second measuring run leads to a final map such that through the trajectory program a punctual source gave at the target, on the focal plane an image of 0.4 mm width, that is the expected accuracy. (fig. 8)

Most of the first results of this spectrometry experience are summed up in our third reference and published in these conference proceedings.

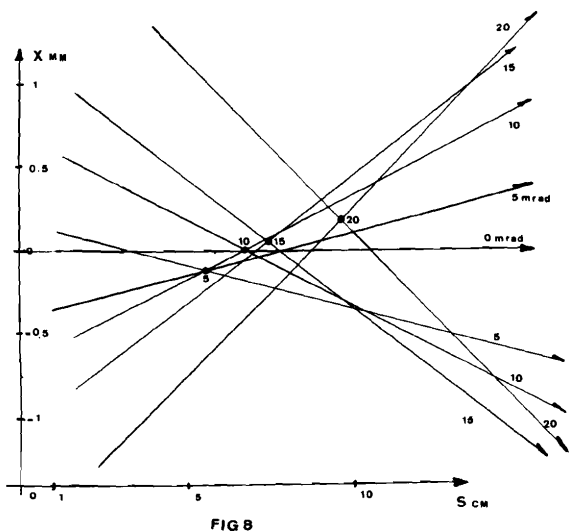


Fig. 8. Image achieved with the shimmed magnet.

References

1. M. Ribes and B. Turck -
Internal report SEDAP/70-126 MM 04.
2. J. Thirion, P. Birien and J. Saudinos-
Note CEA N 1248 (1970).
3. J. Thirion, P. Birien and J. Saudinos-
Proceedings of the IVth Conference on
Magnet Technology - Brookhaven (1972).
4. M. Ribes and B. Turck -
Nucl. Instr. and Meth. 82 (1970) 131.
5. M. Ribes and B. Turck -
Nucl. Instr. and Meth. 93 (1971) 285.
6. B. Turck -
Internal note SEDAP/68-158 MM 01.
7. B. Turck -
Internal report SEDAP/69-146
Spectro 16.
8. C. Eveillard, M. Gueye, G. Laurora,
and B. Turck -
Internal report SEDAP/70-04 Spectro 02
9. B. de Séréville, M. Ohayon and
J.P. Pénicaud -
Proceedings of the IVth Conference
on Magnet Technology - Brookhaven -
(1972)
10. B. de Séréville, M. Ohayon,
J.P. Pénicaud and B. Turck -
Note CEA N 1539 (1972).

